Graphene Oxide Enwrapped Ag/AgX (X = Br, Cl) Nanocomposite as a Highly Efficient Visible-Light Plasmonic Photocatalyst

Mingshan Zhu, Penglei Chen,* and Minghua Liu*

Beijing National Laboratory for Molecular Science, CAS Key Laboratory of Colloid, Interface and Chemical Thermodynamics, Institute of Chemistry, Chinese Academy of Sciences, No. 2 Zhongguancun Beiyijie, Beijing 100190, People's Republic of China

ABSTRACT In this paper, we have reported that well-defined graphene oxide (GO) enwrapped Ag/AgX (X = Br, Cl) nanocomposites, which are composed of Ag/AgX nanoparticles and gauze-like GO nanosheets, could be facilely fabricated *via* a water/oil system. We have shown that thus-synthesized GO-based hybrid nanocomposites could be used as a stable plasmonic photocatalyst for the photodegradation of methyl orange (MO) pollutant under visible-light irradiation. Compared with the corresponding bare Ag/AgX nanospecies, the GO-involved nanocomposites (Ag/AgX/GO) display distinctly enhanced photocatalytic activities. The hybridization of Ag/AgX with GO nanosheets causes the nice adsorptive capacity of Ag/AgX/GO to MO molecules, the smaller size of the Ag/AgX nanoparticles in Ag/AgX/GO, the facilitated charge transfer, and the suppressed recombination of electron–hole pairs in Ag/AgX/GO. It is suggested that these multifactors, resulting from the hybridization of GO, contribute to the enhanced photocatalytic performance observed from Ag/AgX/GO. The investigation likely opens up new possibilities for the development of original yet highly efficient and stable GO-based plasmonic photocatalysts that utilize visible light as an energy source.

KEYWORDS: graphene oxide · hybrid nanocomposite · silver halide · visible-light plasmonic photocatalyst · water/oil system

Graphene oxide (GO), an atomic thick nanosheet of covalently organized two-dimensional lattice of carbon atoms whose basal planes and edges are decorated with various oxygen-containing groups, has recently received considerable attention as a novel cousin of graphene.[1−3] This is essentially owing to its abundant oxygen-containing functional groups such as hydroxyl, epoxide, carbonyl, carboxyl, *etc.*, which favor its nice solubility in solvents and provide fertile opportunities for the construction of GO-based hybrid nanocomposites.[1−3] So far, a paramount of GO-involved nanostructures has been developed aiming at manufacturing sophisticated advanced functional materials for potential applications in electronics and optoelectronics,[4] chemical and biochemical sensors,[5] drug delivery,[6] electrochemical pseudocapacitor,[7] high efficiency catalysis, *etc.*[8−16]

Among various topics, the fabrication of GO-involved catalysts,[8−16] especially those for the photodegradation of pollutants,[12−16] is currently an important issue with particular concern. This is substantially promoted by (i) the excellent transparency, extremely high specific surface area, locally conjugated aromatic system, and unique electronic properties of the graphene-based materials, making them ideal candidates for catalyst carrier or promoter;[8−16] (ii) the severe environmental problem, which requires highly efficient and durable photocatalysts for pollutant abatement. In this regard, several well-defined hybridized nanocomposites in terms of GO and conventional semiconductors, typically exemplified by GO/TiO_2, GO/ZnO, *etc.*, have been recently developed,[12−16] where the formulated hybrids display enhanced photocatalytic performance. Nevertheless, besides the conventional semiconductors,[17−19] it is still highly desirable to develop unique yet highly efficient hybridizers for the visible-light drivable and recyclable GO-based photocatalysts to provide more varied and new opportunities for pollutant elimination and to meet the demands of future environmental issues.

Currently, visible-light-triggered plasmonic photocatalysts have been recognized as one of the most promising alternatives to the traditional photocatalysts.[20−34] It has recently been demonstrated that several silver/silver halide-based (Ag/AgX, X = Br, Cl) nanomaterials could display excellent plasmonic photocatalytic performance in the degradation of pollutants under visible-light irradiation, although AgX species are traditionally used as the primary source

* Address correspondence to chenpl@iccas.ac.cn, liumh@iccas.ac.cn.

Received for review January 9, 2011 and accepted April 27, 2011.

Published online April 27, 2011
10.1021/nn200088x

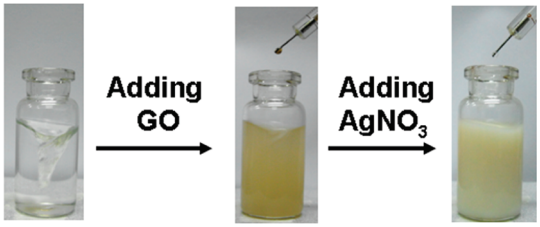

Figure 1. Typical picture indicating the preparation of Ag/AgX/GO hybrid nanocomposites *via* a water/oil system at room temperature.

materials in photographic film and are unstable upon photoillumination.[25−34] Their nice response to visible light could be attributed to the existence of metallic Ag nanoparticles, which give rise to distinct plasmon resonance in the visible region. The boosted photocatalytic activities are ascribed to an efficient charge separation/transfer, which are favored by the existence of metallic Ag nanoparticles in the system.[25−34] However, in these cases, tedious synthesis works, including preparation of Ag/AgX species *via* ion exchange or precipitation *etc.*, are necessary. Consequently, a more facile method is strongly desired.[34]

In this paper, we have newly fabricated an efficient visible-light-driven plasmonic photocatalyst in terms of Ag/AgX/GO nanocomposites, which is excellently stable and could be facilely assembled *via* a water/oil system. In virtue of the incompatibility between water and chloroform, and by taking advantage of bromide and chloride anions that existed in the chloroform solution of cetyltrimethylammonium bromide (CTAB) and cetyltrimethylammonium chloride (CTAC), respectively, we have shown that Ag/AgBr/GO and Ag/AgCl/GO hybrid nanomaterials with well-defined morphologies could be easily assembled *via* a water/oil medium at room temperature, as shown in Figure 1. Importantly, compared with the corresponding bare Ag/AgX nanospecies, the Ag/AgX/GO hybrid nanocomposites display enhanced photocatalytic performance for the photodegradation of methylene orange (MO) dye under visible-light illumination. As far as we know, this might be the first report concerning the assembly of high-performance GO-involved plasmonic photocatalysts. The investigation might open up new possibilities for the development of original yet highly efficient and stable GO-based plasmonic photocatalysts that utilize visible light as an energy source.

RESULTS AND DISCUSSION

Experimentally, as shown in Figure 1, our Ag/AgX/GO hybrid nanocomposites could be facilely fabricated by adding an aqueous solution of GO and silver nitrate ($AgNO_3$) dropwise into a chloroform solution of surfactants (CATB or CTAC) successively. The corresponding Ag/AgX species could also be facilely obtained *via* an allied process when only $AgNO_3$ but no GO nanosheet was involved. An opaque system with a yellowish and white yellowish color was obtained in sequence, respectively, after the dropwise addition of an aqueous solution of GO nanosheet and $AgNO_3$ into a chloroform solution of surfactants. This is owing to the incompatibility between water and chloroform and the formation of the target nanostructures.[35] The morphologies of the produced nanostructures were characterized by scanning electron microscopy (SEM), as shown in Figure 2. It can be seen that nanoparticles with an average diameter of *ca.* 500 nm could be obtained in the cases of Ag/AgX nanospecies. Well-defined nanospheres, whose average diameter is *ca.* 200 nm and whose surface is distinctly enwrapped with gauze-like GO nanosheets, could be obtained in the cases of Ag/AgX/GO hybrid nanocomposites. The smaller size of Ag/AgX nanospheres observed from the Ag/AgX/GO systems compared with that of the corresponding Ag/AgX systems might be due to the existence of GO nanosheets in these systems because it has recently been demonstrated that GO, an unconventional amphiphile, could act as a surfactant in an oil−water system,[36] which might be able to further improve the dispersibility of water phase in the chloroform solution of surfactants.

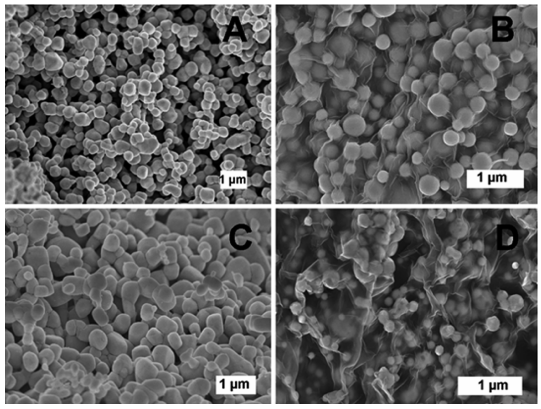

Figure 2. Typical SEM images of the synthesized Ag/AgBr (A), Ag/AgBr/GO (B), Ag/AgCl (C), and Ag/AgCl/GO (D) nanospecies.

Generally, bare AgX species could only display distinct absorption in the ultraviolet region but negligible absorption in the visible region.[25,26,28,29,34] Thus-produced nanostructures were subjected to the UV−vis spectral measurements. As shown in Figure 3, it can be seen that all of the investigated Ag/AgX-involved species display strong absorption both in the ultraviolet and visible regions. This suggests the existence of metallic Ag species in all of our samples, which could arouse plasmon resonance absorptions in the visible region.[25−30,34] The absorption spectra of Ag/AgX/GO nanocomposites display a distinct absorption of GO at *ca.* 238 nm, confirming the existence of GO sheets in these systems.[37] In order to verify the hybridization of Ag/AgX with GO in Ag/AgX/GO systems, their Fourier transform infrared spectra (FT-IR) together with that of

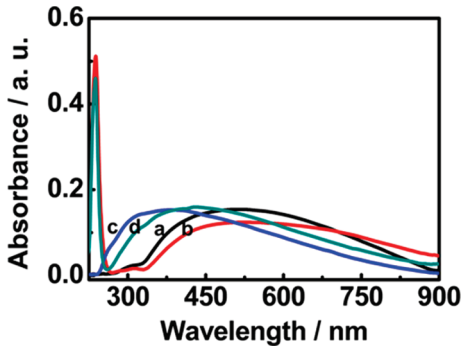

Figure 3. Typical UV−vis spectra of Ag/AgBr (a), Ag/AgBr/GO (b), Ag/AgCl (c), and Ag/AgCl/GO (d) nanospecies.

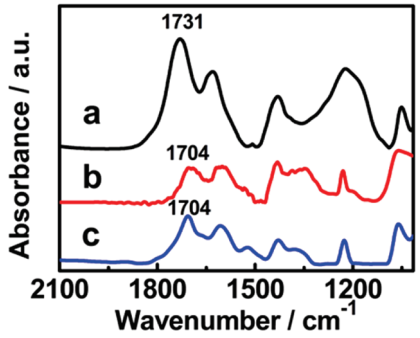

Figure 4. Typical FT-IR spectra of the powdery GO (a), Ag/AgBr/GO (b), and Ag/AgCl/GO (c) nanostructures.

powdery GO were measured as presented in Figure 4. It could be seen that the powdery GO displays several characteristic bands at 1731, 1625, 1425, 1222, and 1051 cm^{-1}, which are ascribed to the C═O carbonyl stretching, the vibrations of the adsorbed water molecules, the skeletal vibrations of unoxidized graphitic domains, the O−H deformation vibration, and the C−OH and C−O stretching, respectively.[38,39] The C═O carbonyl stretching band at 1731 cm^{-1} observed from the powdery GO shifts to lower wavenumber, 1704 cm^{-1}, for Ag/AgX/GO systems, indicating the evident interactions between the Ag/AgX nanoparticles and GO nanosheet.[40,41] This result confirms the successful hybridization between Ag/AgX nanospheres and GO nanosheets.

The photocatalytic performance of our Ag/AgX-involved nanocomposites in terms of photodegradation of MO molecules under visible-light irradiation was investigated. As it is known, the adsorptive capacity of catalysts for the pollutant molecules is one of the crucial factors required for nice photocatalytic activity.[12,14,42] A dark adsorption was carried out for 30 min prior to the visible-light irradiation to achieve an equilibrium adsorption state. As shown in Figure S1 in the Supporting Information, compared to the bare Ag/AgX nanospecies, the corresponding Ag/AgX/GO hybrid nanocomposites exhibit a higher adsorptive capacity for MO molecules. This could be attributed

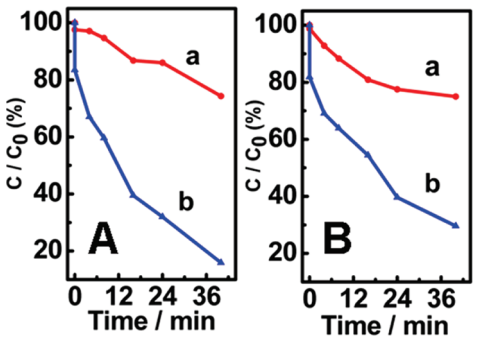

Figure 5. (A) Photocatalytic activities of Ag/AgBr (a) and Ag/AgBr/GO (b) nanospecies for photodegradation of MO molecules under visible-light irradiation. (B) Those of Ag/AgCl (a) and Ag/AgCl/GO (b) nanospecies.

to the hybridization of GO nanosheets in these systems, which have been proven to facilitate the adsorption of pollutant molecules, owing to the noncovalent intermolecular $\pi-\pi$ interactions between the pollutant molecules and GO-based hybrids.[12,14,16] As presented in Figure S1, the photodegradation of MO was monitored by measuring its real-time UV−vis absorption spectra, where it is found that the absorption of MO at 463 nm decreases continuously with increasing irradiation time. These results suggest that our Ag/AgX-involved nanostructures could work as plasmonic photocatalysts[25−34] for the photodegradation of MO pollutant.

As shown in Figure 5, when the bare Ag/AgX nanospecies are employed as photocatalysts, *ca.* 25% of MO molecules are decomposed after being irradiated for 40 min under our experimental conditions. In contrast, when Ag/AgBr/GO and Ag/AgCl/GO hybrid nanocomposites are used as photocatalysts, *ca.* 85 and 71% MO molecules are decomposed, respectively, under similar experimental conditions. Accordingly, it could be seen that the photocatalytic activities of Ag/AgBr/GO and Ag/AgCl/GO hybrid nanocomposites are essentially higher than those of the corresponding bare Ag/AgX nanospecies by a factor of *ca.* 3.5 and 2.8, respectively. This suggests that the photocatalytic performance of our plasmonic photocatalysts, Ag/AgX, could be distinctly enhanced *via* hybridization with GO nanosheets. Moreover, the stability of our Ag/AgX/GO-based plasmonic photocatalysts was evaluated in terms of performing the MO bleaching reactions repeatedly five times, as shown in Figure 6. The photocatalytic efficiency only displays slight decrease without significant loss of activities after the reaction is performed consecutively five times. The morphology of the catalysts does not display significant changes after the bleaching reactions, as suggested by the SEM shown in Figure S2 in the Supporting Information. These results suggest that our Ag/AgX/GO hybrid nanocomposites are efficient and stable visible-light plasmonic photocatalysts[25−34] for the photocatalytic

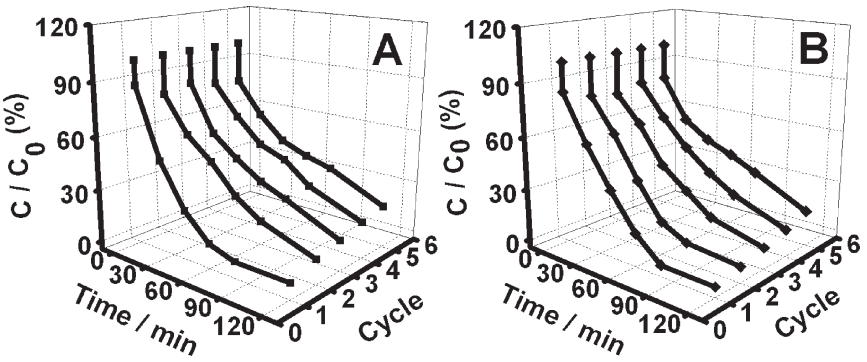

Figure 6. Five consecutive cycling photodegradation curves of MO dye over Ag/AgBr/GO (A) and Ag/AgCl/GO (B) hybrid nanocomposites, respectively.

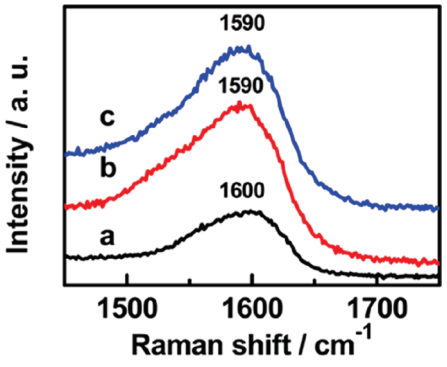

Figure 7. Typical Raman spectra of the G-band of the powdery GO naonsheets (a), Ag/AgBr/GO (b), and Ag/AgCl/GO (c) hybrid nanocomposites.

decolorization of MO molecules. The slight decrease of the activity during the recycling reactions could be attributed to the loss of some of the catalysts during the photocatalytic performances since the dosage of the catalysts is very small, as suggested by other researchers.[43] The loss of the catalysts might also be due to the nice dispersibility of Ag/AgX/GO species in aqueous solutions, which is favored by the nice solubility of GO nanosheets in aqueous systems.[3,36] This makes it easy for some of the catalyst to be taken away from the photocatalytic system during the real-time sampling procedure.

As it is widely known, an efficient charge separation/transfer is crucial for the enhancement of the photocatalytic activities.[12,17−19] It has been shown that a novel hybrid nanocompsite, Ag/AgX/TiO_2, could exhibit improved photocatalytic activities, where it is suggested that the facilitated charge separation/transfer, favors its excellent performance.[32] In this case, TiO_2 and Ag/AgX species work as electron acceptor and electron donor, respectively. On the other hand, GO/TiO_2 hybrid nanocomposites have more recently been reported to be superior photocatalysts in photodegradation of pollutant molecules. Herein, their excellent photocatalytic performance has been attributed to the efficient electron transferring from TiO_2 to GO species, where GO and TiO_2 have been verified to act as electron acceptor and electron donor, respectively.[12] Thus, it is reasonable to assume that a reinforced charge separation/transfer might be achieved in our Ag/AgX/GO hybrid nanocomposites, where GO and Ag/AgX might act as electron acceptor and electron donor, respectively.

As known, the occurrence of charge transfer between GO and the hybridized components could be verified by the Raman spectra, where it has been demonstrated that the G-band of GO nanosheets shifts to lower frequency when GO is hybridized with an electron donor component, while it shifts to higher frequency when an electron acceptor component is hybridized.[44−46] The Raman spectra of our Ag/AgX/GO hybrid nanocomposites together with that of powdery GO nanosheets were measured. As shown in Figure 7, a G-band at *ca.* 1600 cm^{-1}, which is typical Raman features of GO nanosheets, could be observed from the original powdery GO species.[47] In contrast, the G-band shifts by 10 cm^{-1} to a lower frequency at 1590 cm^{-1} for Ag/AgX/GO hybrid nanocomposites. This result confirms the occurrence of charge transfer between Ag/AgX and GO of our GO-based hybrid nanocomposites, where Ag/AgX and GO species work as electron donor and electron acceptor components, respectively.[44−46]

Moreover, the X-ray photoelectron spectroscopy (XPS) of our Ag/AgX/GO hybrid nanocomposites together with that of the bare Ag/AgX nanospecies was examined, as shown in Figure 8. For Ag/AgX nanomaterials, two bands at *ca.* 367.5 and 373.5 eV, ascribed to Ag $3d_{5/2}$ and Ag $3d_{3/2}$ binding energies,[26−28] respectively, are observed. These two bands could be further deconvoluted into two peaks, respectively, at 367.5, 368.8 eV and 373.5, 374.6 eV, where the bands at 367.5 and 373.5 eV are attributed to the Ag^+ of AgX, and those at 368.8 and 374.6 eV are ascribed to the metallic Ag^0. Similar results are reported by other researchers.[26−28] The calculated surface mole ratio of the metallic Ag^0 to Ag^+ is *ca.* 1:16. These results verify the existence of metallic Ag^0 in our Ag/AgX species, as suggested by the UV−vis spectra. In the cases of

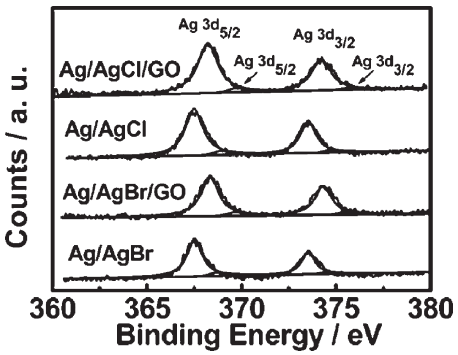

Figure 8. Typical XPS spectra of Ag 3d of Ag/AgX and Ag/AgX/GO nanostructures.

GO-based hybrid nanocomposites, Ag/AgX/GO, the Ag $3d_{5/2}$ and Ag $3d_{3/2}$ peaks shift to higher binding energies to 368.3 and 374.3 eV, respectively. The deconvolution of these two bands gives out peaks at 368.3, 369.7 eV and 374.3, 375.6 eV, respectively. Those at 368.3 and 374.3 eV could be ascribed to the Ag^+ of AgX, while those at 369.7 and 375.6 eV are ascribed to the metallic Ag^0, all of which display nearly 1 eV shift to higher binding energy compared with those of the corresponding bare Ag/AgX species. These results confirm the existence of metallic Ag^0 in our Ag/AgX/GO hybrid nanocomposites, and it further verifies that the Ag/AgX species of our GO-based hybrid nanocomposites might indeed work as electron donor when hybridized with GO nanosheets.[48] Similar to that of Ag/AgX species, the calculated surface mole ratio of metallic Ag^0 to Ag^+ in GO-based hybrid nanocomposites is also *ca.* 1:16.

As shown Figures S3−S6 in the Supporting Information, both the Raman spectra and XPS spectra of our Ag/AgX/GO hybrid nanocomposites only display slight changes after the photocatalytic performance. These results further confirm that our Ag/AgX/GO nanocomposites have nice stability during the photocatalytic operations.

On the basis of the above-mentioned experimental facts and analysis, we could propose an explanation for the enhanced photocatalytic performance observed from our Ag/AgX/GO hybrid nanocomposites. The distinct plasmon absorption in the visible region, which is aroused by the existing metallic Ag^0 species, makes our photocatalysts visible-light drivable.[25−34] During the dark adsorption, MO molecules are inclined to be adsorbed on Ag/AgX/GO hybrid nanocomposites, through noncovalent $\pi-\pi$ intermolecular interactions.[12,14,16] This nice adsorptive capacity of Ag/AgX/GO to MO molecules might contribute partially to the enhanced photocatalytic activity of the Ag/AgX/GO hybrid species, as suggested by other researchers.[12,14,16,42] On the other hand, the size of Ag/AgX nanospecies in the case of Ag/AgX/GO hybrid nanocomposites is smaller than that of bare Ag/AgX nanospecies, which might also contribute partially to a nice photocatalytic performance.[34] Moreover, as deduced from refs 12 and 32 and suggested by our Raman spectra and XPS spectra, Ag/AgX and GO components might serve as electron donor and electron acceptor, respectively, in the Ag/AgX/GO hybrid nanocomposites. As a result, the photogenerated electrons could migrate into GO nanosheets through a percolation process during the photocatalytic performance.[12,49] This could essentially promote the charge separation/transfer and thus suppress the charge recombination of electron−hole pairs, enhancing the photocatalytic performance.[12−16,25−30,34] It could be seen that the hybridization of Ag/AgX with GO nanosheets favors the nice adsorptive capacity of Ag/AgX/GO to MO molecules, the smaller size of the Ag/AgX nanoparticles in Ag/AgX/GO, the facilitated charge transfer, and the suppressed recombination of electron−hole pairs in Ag/AgX/GO, which might conjointly contribute to the enhanced photocatalytic performance.

CONCLUSION

In summary, we have shown that a unique yet highly efficient visible-light-driven plasmonic photocatalyst based on Ag/AgX/GO hybrid nanocomposites with enhanced photocatalytic activity and excellent stability could be facilely produced *via* a water/oil system at room temperature. It is suggested that the nice adsorptive capacity of Ag/AgX/GO nanospecies to MO molecules, the smaller size of Ag/AgX nanoparticle in the GO-involved hybrid nanocomposites, the reinforced charge transfer, and the suppressed recombination of electron−hole pairs in Ag/AgX/GO, which result from hybridization of Ag/AgX with GO nanosheets, contribute to the enhanced photocatalytic activity. The results indicate that our photocatalysts have potential application for pollutant abatement. As far as we know, this might be the first report concerning the assembly of high-performance GO-involved plasmonic photocatalysts. The investigation opens up new opportunities for the development of new GO-involved plasmonic photocatalysts that utilize visible light as an energy source.

METHODS

Materials. Silver nitrate ($AgNO_3$, Beijing Yili Fine Chemical Co., Ltd., 99.5%), cetyltrimethylammonium bromide (CTAB, Alfa Aesar, 99%), cetyltrimethylammonium chloride (CTAC, Alfa Aesar, 95%), and graphite powder (Alfa Aesar, 325mesh, 99.9995%) were used as received without further treatments.

Preparation of Graphene Oxide (GO) Nanosheets. GO nanosheets were prepared by chemical exfoliation of the graphite powder

by using a modified Hummers' method.[50,51] Typically, 1 g of graphite powder was added to 23 mL of cooled (0 °C), concentrated H_2SO_4, after which 3 g of $KMnO_4$ was added gradually under vigorous stirring. During this process, the temperature of the mixture was maintained below 20 °C using an ice bath. The mixture was further stirred at 35 °C for 30 min. Subsequently, 46 mL of ultrapure Milli-Q water was slowly added to the system, and the temperature of the system was increased to 98 °C. The mixture was maintained at that temperature for 15 min. The reaction was terminated by adding 140 mL of ultrapure Milli-Q water, which was followed by 10 mL of 30% H_2O_2 solution. The solid product was separated by centrifugation and washed repeatedly with 5% HCl solution until sulfate could not be detected with $BaCl_2$. Then the sample was dried in a vacuum oven at 25 °C overnight.

To obtain GO nanosheets dispersed in water, 100 mg of thus-synthesized dried solid product was added to 50 mL of ultrapure Milli-Q water, after which the system was treated with an ultrasonic homogenizer (Ningbo Scientz Biotechnology Co., Ltd., Scientz-II D, frequency = 20 kHz, output power = 400 W) for 1 h. Subsequently, the suspension was repeatedly treated by high-speed centrifugation (8000 rpm, 5 min) four times to remove impurities. The mass concentration of the obtained aqueous GO nanosheet dispersion was estimated to be 1 mg mL^{-1}.

Synthesis of Ag/AgX/GO and Ag/AgX Nanostructures. In a typical process, a 400 μL aqueous solutions of GO nanosheet (1 mg mL^{-1}) and a 500 μL aqueous solution of $AgNO_3$ (0.1 mol L^{-1}) were added dropwise into a 10 mL chloroform solution of CTAB or CTAC (8.23×10^{-3} mol L^{-1}) successively within 10 min under magnetic stirring. The vigorous stirring was maintained for another 20 min, after which a milky dispersion containing Ag/AgX/GO hybrid nanocomposites was obtained. The resulting white yellowish solids were collected by centrifugation (10 000 rpm, 10 min) and washed thoroughly first with ethanol and then with ultrapure Milli-Q water by repeating centrifugations. When only $AgNO_3$ species but no GO nanosheets were employed, the corresponding Ag/AgX species could also be thus synthesized *via* a parallel process. Note that the above-mentioned synthesis works were performed without being protected from the ambient light. On the other hand, we also carried out our synthesis works in a strictly darkened room, where there was only a weak infrared lamp on the wall. In these cases, as shown in Figure S7 in the Supporting Information, thus-obtained products display almost no plasmon resonance absorptions in the visible region, suggesting that the generation of the Ag^0 species could be nearly forbidden under this circumstance. This deduction was further confirmed by the XPS spectra of thus-synthesized catalysts, where only distinct bands attributed to Ag^+ but almost no bands ascribed to Ag^0 could be detected, as shown in Figure S8. This result confirms that the generation of Ag^0 species in our catalysts might be result from the ambient light.

Photocatalytic Performance. In a typical performance, photocatalysts were dispersed in a 12 mL of aqueous solution of methyl orange (MO) dye (15 mg L^{-1}). The dispersion was kept in the dark for 30 min for dark adsorption experiment, after which the photodegradation was carried out. The dark adsorption time was designed to be 30 min because it was found that, when a longer adsorption time, say 48 h, was employed, similar results were obtained. The light source was a 500 W xenon arc lamp installed in a laboratory lamp housing system (CHF-XM35-500 W, Beijing Trusttech Co. Ltd., China). Before entering the reactor, the light passed through a 10 cm water filter and a UV cutoff filter (>400 nm). Aliquots of dispersion (0.3 mL) were taken out from the reaction system for the real-time investigation. For the evaluation of the photocatalytic activities, C is the concentration of MO molecule at a real-time t, and C_0 is that in the MO solution immediately before it is kept in the dark.[25] For comparison, blank experiments without illumination have also been carried out. As shown in Figure S9 in the Supporting Information, negligible degradation of MO molecules could be observed in these cases.

The amount of our photocatalysts employed for the photocatalytic performance was estimated by drying the products at room temperature under vacuum for 72 h. We found that the amount of Ag/AgBr, Ag/AgBr/GO, Ag/AgCl, and Ag/AgCl/GO was evaluated to be *ca.* 7.7, 7.4, 7.4, and 7.3 mg, respectively. Note that the amount of Ag/AgBr/GO (7.4 mg) and Ag/AgCl/GO (7.3 mg) species was unexpectedly a little bit smaller than that of Ag/AgBr (7.7 mg) and Ag/AgCl (7.4 mg) species, respectively. Operationally, during our synthesis process, we found that supernatant with a white yellowish color was always inevitably taken out during the washing of Ag/AgX/GO species, no matter how large the centrifugation speed was. This could naturally result in a loss of some of the formed Ag/AgX/GO nanospecies. The loss of the Ag/AgX/GO might be due to their nice dispersibility in aqueous solutions, which is promoted by the good solubility of GO nanosheets in aqueous systems.[3,36] This makes it easy for some of the Ag/AgX/GO species to be taken away with supernatant during the washing process, resulting in the smaller amount of the obtained Ag/AgX/GO species. Accordingly, from this point of view, the photocatalytic activity of Ag/AgX/GO compared with that of the corresponding Ag/AgX species is actually at a disadvantage owing to the smaller amount of their virtual Ag/AgX content, although the GO's content in Ag/AgX/GO species could not be estimated at the present stage.

Apparatus and Measurements. JASCO UV-550 and JASCO IR-660 spectrometers were employed for the UV−vis and FT-IR spectral measurements, respectively. The SEM measurements were performed by using a Hitachi S-4800 system. X-ray photoelectron spectroscopy (XPS) was performed on an ESCALab220i-XL electron spectrometer from VG Scientific using 300 W Al Kα radiation. The binding energies were referenced to the C1s line at 284.8 eV from adventitious carbon. The Raman spectra were recorded on a Renishaw inVia plus Raman microscope using a 514.5 nm argon ion laser. All of the measurements were carried out at room temperature.

Acknowledgment. We appreciate NSFC (20773141 and 21021003), National Key Basic Research Project of China (2007CB808005 and 2011CB932301), and Chinese Academy of Sciences. The authors are grateful to Prof. Wanhong Ma and Dr. Chuncheng Chen from the Institute of Chemistry, Chinese Academy of Sciences, for their profound discussions.

Supporting Information Available: Real-time absorption spectra of MO dye during the photodegradation process over various photocatalysts and the corresponding SEM images, Raman spectra, and XPS spectra of the GO-based hybrid nanocomposites after the photocatalytic degradation of MO dye under visible-light irradiation, *etc.* This material is available free of charge *via* the Internet at http://pubs.acs.org.

REFERENCES AND NOTES

1. Eda, G.; Chhowalla, M. Chemically Derived Graphene Oxide: Towards Large-Area Thin-Film Electronics and Optoelectronics. *Adv. Mater.* **2010**, *22*, 2392–2415.
2. Steurer, P.; Wissert, R.; Thomann, R.; Mülhaupt, R. Functionalized Graphenes and Thermoplastic Nanocomposites Based upon Expanded Graphite Oxide. *Macromol. Rapid Commun.* **2009**, *30*, 316–327.
3. Dreyer, D. R.; Park, S.; Bielawski, C. W.; Ruoff, R. S. The Chemistry of Graphene Oxide. *Chem. Soc. Rev.* **2010**, *39*, 228–240.
4. Zhuang, X.-D.; Chen, Y.; Liu, G.; Li, P.-P.; Zhu, C.-X.; Kang, E.-T.; Neoh, K.-G.; Zhang, B.; Zhu, J.-H.; Li, Y.-X. Conjugated-Polymer-Functionalized Graphene Oxide: Synthesis and Nonvolatile Rewritable Memory Effect. *Adv. Mater.* **2010**, *22*, 1731–1735.
5. Balapanuru, J.; Yang, J.-X.; Xiao, S.; Bao, Q.; Jahan, M.; Polavarapu, L.; Wei, J.; Xu, Q.-H.; Loh, K. P. A Graphene Oxide−Organic Dye Ionic Complex with DNA-Sensing and Optical-Limiting Properties. *Angew. Chem., Int. Ed.* **2010**, *49*, 6549–6553.
6. Liu, Z.; Robinson, J. T.; Sun, X.; Dai, H. PEGylated Nano-Graphene Oxide for Delivery of Insoluble Cancer Drugs. *J. Am. Chem. Soc.* **2008**, *130*, 10876–10877.
7. Wang, H.; Casalongue, H. S.; Liang, Y.; Dai, H. $Ni(OH)_2$ Nanoplates Grown on Graphene as Advanced Electrochemical

Pseudocapacitor Materials. *J. Am. Chem. Soc.* **2010**, *132*, 7472–7477.
8. Scheuermann, G. M.; Rumi, L.; Steurer, P.; Bannwarth, W.; Mülhaupt, R. Palladium Nanoparticles on Graphite Oxide and Its Functionalized Graphene Derivatives as Highly Active Catalysts for the Suzuki–Miyaura Coupling Reaction. *J. Am. Chem. Soc.* **2009**, *131*, 8262–8270.
9. Zhou, Y.-G.; Chen, J.-J.; Wang, F.-B.; Sheng, Z.-H.; Xia, X.-H. A Facile Approach to the Synthesis of Highly Electroactive Pt Nanoparticles on Graphene as an Anode Catalyst for Direct Methanol Fuel Cells. *Chem. Commun.* **2010**, *46*, 5951–5953.
10. Li, Y.; Fan, X.; Qi, J.; Ji, J.; Wang, S.; Zhang, G.; Zhang, F. Palladium Nanoparticle–Graphene Hybrids as Active Catalysts for the Suzuki Reaction. *Nano Res.* **2010**, *3*, 429–437.
11. Ng, Y. H.; Iwase, A.; Kudo, A.; Amal, R. Reducing Graphene Oxide on a Visible-Light $BiVO_4$ Photocatalyst for an Enhanced Photoelectrochemical Water Splitting. *J. Phys. Chem. Lett.* **2010**, *1*, 2607–2612.
12. Zhang, H.; Lv, X.; Li, Y.; Wang, Y.; Li, J. P25–Graphene Composite as a High Performance Photocatalyst. *ACS Nano* **2010**, *4*, 380–386.
13. Chen, C.; Cai, W.; Long, M.; Zhou, B.; Wu, Y.; Wu, D.; Feng, Y. Synthesis of Visible-Light Responsive Graphene Oxide/TiO_2 Composites with p/n Heterojunction. *ACS Nano* **2010**, *4*, 6425–6432.
14. Liu, J.; Bai, H.; Wang, Y.; Liu, Z.; Zhang, X.; Sun, D. D. Self-Assembling TiO_2 Nanorods on Large Graphene Oxide Sheets at a Two-Phase Interface and Their Anti-recombination in Photocatalytic Applications. *Adv. Funct. Mater.* **2010**, *20*, 4175–4181.
15. Ng, Y. H.; Lightcap, I. V.; Goodwin, K.; Matsumura, M.; Kamat, P. V. To What Extent Do Graphene Scaffolds Improve the Photovoltaic and Photocatalytic Response of TiO_2 Nanostructured Films?. *J. Phys. Chem. Lett.* **2010**, *1*, 2222–2227.
16. Liang, Y.; Wang, H.; Casalongue, H. S.; Chen, Z.; Dai, H. TiO_2 Nanocrystals Grown on Graphene as Advanced Photocatalytic Hybrid Materials. *Nano Res.* **2010**, *3*, 701–705.
17. Chen, C.; Ma, W.; Zhao, J. Semiconductor-Mediated Photodegradation of Pollutants under Visible-Light Irradiation. *Chem. Soc. Rev.* **2010**, *39*, 4206–4219.
18. Hoffmann, M. R.; Martin, S. T.; Choi, W.; Bahnemannt, D. W. Environmental Applications of Semiconductor Photocatalysis. *Chem. Rev.* **1995**, *95*, 69–96.
19. Yang, D.; Liu, H.; Zheng, Z.; Yuan, Y.; Zhao, J.; Waclawik, E. R.; Ke, X.; Zhu, H. An Efficient Photocatalyst Structure: TiO(2)(B) Nanofibers with a Shell of Anatase Nanocrystals. *J. Am. Chem. Soc.* **2009**, *131*, 17885–17893.
20. Awazu, K.; Fujimaki, M.; Rockstuhl, C.; Tominaga, J.; Murakami, H.; Ohki, Y.; Yoshida, N.; Watanabe, T. A Plasmonic Photocatalyst Consisting of Silver Nanoparticles Embedded in Titanium Dioxide. *J. Am. Chem. Soc.* **2008**, *130*, 1676–1680.
21. Hu, C.; Peng, T.; Hu, X.; Nie, Y.; Zhou, X.; Qu, J.; He, H. Plasmon-Induced Photodegradation of Toxic Pollutants with Ag–AgI/Al_2O_3 under Visible-Light Irradiation. *J. Am. Chem. Soc.* **2010**, *132*, 857–862.
22. Elahifard, M. R.; Rahimnejad, S.; Haghighi, S.; Gholami, M. R. Apatite-Coated Ag/AgBr/TiO_2 Visible-Light Photocatalyst for Destruction of Bacteria. *J. Am. Chem. Soc.* **2007**, *129*, 9552–9553.
23. Chen, X.; Zheng, Z.; Ke, X.; Jaatinen, E.; Xie, T.; Wang, D.; Guo, C.; Zhao, J.; Zhu, H. Supported Silver Nanoparticles as Photocatalysts under Ultraviolet and Visible Light Irradiation. *Green Chem.* **2010**, *12*, 414–419.
24. Zhu, H.; Chen, X.; Zheng, Z.; Ke, X.; Jaatinen, E.; Zhao, J.; Guo, C.; Xie, T.; Wang, D. Mechanism of Supported Gold Nanoparticles as Photocatalysts under Ultraviolet and Visible Light Irradiation. *Chem. Commun.* **2009**, 7524–7526.
25. Wang, P.; Huang, B.; Qin, X.; Zhang, X.; Dai, Y.; Wei, J.; Whangbo, M. Ag@AgCl: A Highly Efficient and Stable Photocatalyst Active under Visible Light. *Angew. Chem., Int. Ed.* **2008**, *47*, 7931–7993.
26. Wang, P.; Huang, B.; Qin, X.; Zhang, X.; Dai, Y.; Whangbo, M. Ag/AgBr/WO_3•H_2O: Visible-Light Photocatalyst for Bacteria Destruction. *Inorg. Chem.* **2009**, *48*, 10697–10702.
27. Wang, P.; Huang, B.; Lou, Z.; Zhang, X.; Qin, X.; Dai, Y.; Zheng, Z.; Wang, X. Synthesis of Highly Efficient Ag@AgCl Plasmonic Photocatalysts with Various Structures. *Chem.—Eur. J.* **2010**, *16*, 538–544.
28. Wang, P.; Huang, B.; Zhang, Q.; Zhang, X.; Qin, X.; Dai, Y.; Zhan, J.; Yu, J.; Liu, H.; Lou, Z. Highly Efficient Visible Light Plasmonic Photocatalyst Ag@Ag (Br,I). *Chem.—Eur. J.* **2010**, *16*, 10042–10047.
29. Wang, P.; Huang, B.; Zhang, X.; Qin, X.; Jin, H.; Dai, Y.; Wang, Z.; Wei, J.; Zhan, J.; Wang, S.; *et al.* Highly Efficient Visible-Light Plasmonic Photocatalyst Ag@AgBr. *Chem.—Eur. J.* **2009**, *15*, 1821–1824.
30. Wang, P.; Huang, B.; Zhang, X.; Qin, X.; Dai, Y.; Jin, H.; Wei, J.; Whangbo, M. Composite Semiconductor $H_2WO_4 \cdot H_2O$/AgCl as an Efficient and Stable Photocatalyst under Visible Light. *Chem.—Eur. J.* **2008**, *14*, 10543–10546.
31. Bi, Y.; Ye, J. Direct Conversion of Commercial Silver Foils into High Aspect Ratio AgBr Nanowires with Enhanced Photocatalytic Properties. *Chem.—Eur. J.* **2010**, *16*, 10327–10311.
32. Yu, J.; Dai, G.; Huang, B. Fabrication and Characterization of Visible-Light-Driven Plasmonic Photocatalyst Ag/AgCl/TiO_2 Nanotube Arrays. *J. Phys. Chem. C* **2009**, *113*, 16394–16401.
33. Zang, Y.; Farnood, R. Photocatalytic Activity of AgBr/TiO_2 in Water under Simulated Sunlight Irradiation. *Appl. Catal. B* **2008**, *79*, 334–340.
34. An, C.; Peng, S.; Sun, Y. Facile Synthesis of Sunlight-Driven AgCl:Ag Plasmonic Nanophotocatalyst. *Adv. Mater.* **2010**, *22*, 2570–2574.
35. Qiu, Y.; Chen, P.; Liu, M. Evolution of Various Porphyrin Nanostructures *via* an Oil/Aqueous Medium: Controlled Self-Assembly, Further Organization, and Supramolecular Chirality. *J. Am. Chem. Soc.* **2010**, *132*, 9644–9652.
36. Kim, J.; Cote, L. J.; Kim, F.; Yuan, W.; Shull, K. R.; Huang, J. Graphene Oxide Sheets at Interfaces. *J. Am. Chem. Soc.* **2010**, *132*, 8180–8186.
37. Li, D.; Müller, M. B.; Gilje, S.; Kaner, R. B.; Wallace, G. G. Processable Aqueous Dispersions of Graphene Nanosheets. *Nat. Nanotechnol.* **2008**, *3*, 101–105.
38. Zhang, D.–D.; Zu, S.–Z.; Han, B.–H. Inorganic–Organic Hybrid Porous Materials Based on Graphite Oxide Sheets. *Carbon* **2009**, *47*, 2993–3000.
39. Titelman, G. I.; Gelman, V.; Bron, S.; Khalfin, R. L.; Cohen, Y.; Bianco-Peled, H. Characteristics and Microstructure of Aqueous Colloidal Dispersions of Graphite Oxide. *Carbon* **2005**, *43*, 641–649.
40. Petroski, J.; El-Sayed, M. A. FTIR Study of the Adsorption of the Capping Material to Different Platinum Nanoparticle Shapes. *J. Phys. Chem. A* **2003**, *107*, 8371–8375.
41. Yang, P.; Zhang, W.; Du, Y.; Wang, X. Hydrogenation of Nitrobenzenes Catalyzed by Platinum Nanoparticle Core–Polyaryl Ether Trisacetic Acid Ammonium Chloride Dendrimer Shell Nanocomposite. *J. Mol. Catal. A* **2006**, *260*, 4–10.
42. Morales, W.; Cason, M.; Aina, O.; De Tacconi, N. R.; Rajeshwar, K. Combustion Synthesis and Characterization of Nanocrystalline WO_3. *J. Am. Chem. Soc.* **2008**, *130*, 6318–6319.
43. Li, Y.; Ding, Y. Porous AgCl/Ag Nanocomposites with Enhanced Visible Light Photocatalytic Properties. *J. Phys. Chem. C* **2010**, *114*, 3175–3179.
44. Das, A.; Pisana, S.; Chakraborty, B.; Piscanec, S.; Saha, S. K.; Waghmare, U. V.; Novoselov, K. S.; Krishnamurthy, H. R.; Geim, A. K.; Ferrari, A. C.; *et al.* Monitoring Dopants by Raman Scattering in an Electrochemically Top-Gated Graphene Transistor. *Nat. Nanotechnol.* **2008**, *3*, 210–215.
45. Xu, Y.; Wu, Q.; Sun, Y.; Bai, H.; Shi, G. Three-Dimensional Self-Assembly of Graphene Oxide and DNA into Multifunctional Hydrogels. *ACS Nano* **2010**, *4*, 7358–7362.
46. Ghosh, A.; Rao, K. V.; George, S. J.; Rao, C. N. R. Noncovalent Functionalization, Exfoliation, and Solubilization of Graphene

in Water by Employing a Fluorescent Coronene Carboxylate. *Chem.—Eur. J.* **2010**, *16*, 2700–2704.
47. Stankovich, S.; Dikin, D. A.; Piner, R. D.; Kohlhaas, K. A.; Kleinhammes, A.; Jia, Y.; Wu, Y.; Nguyen, S. T.; Ruoff, R. S. Synthesis of Graphene-Based Nanosheets *via* Chemical Reduction of Exfoliated Graphite Oxide. *Carbon* **2007**, *45*, 1558–1565.
48. Briggs, D. *Handbook of X-ray and Ultraviolet Photoelectron Spectroscopy*; Heyden: London, 1977.
49. Wang, X.; Zhi, L.; Müllen, K. Transparent, Conductive Graphene Electrodes for Dye-Sensitized Solar Cells. *Nano Lett.* **2008**, *8*, 323–327.
50. Hummers, W. S.; Offeman, R. E. Preparation of Graphitic Oxide. *J. Am. Chem. Soc.* **1958**, *80*, 1339–1339.
51. Nethravathi, C.; Rajamathi, M. Chemically Modified Graphene Sheets Produced by the Solvothermal Reduction of Colloidal Dispersions of Graphite Oxide. *Carbon* **2008**, *46*, 1994–1998.